$Ru(bpy)_2^{2+}$ and $Os(bpy)_2^{2+}$ Complexes of Large Polyaza Cavity-Shaped Ligands

Randolph P. Thummel,* Darwin Williamson, and Christophe Hery

Department of Chemistry, University of Houston, Houston, Texas 77204-5641

Received June 19, 1992

The Friedländer condensation of cyclic 1,2-diketones with 2-amino-5,6-dihydro-1,10-phenanthroline-3-carboxaldehyde provides a series of hexaaza cavity-shaped molecules **2a–c**. Reaction with $Ru(bpy)_2Cl_2$ (where bpy = 2,2′-bipyridine) incorporates Ru(II) into a distal bidentate site. For ligands which are significantly nonplanar, a second Ru(II) or Os(II) nucleus can similarly be incorporated into the remaining distal site. The use of bpy-d_8 as an auxilliary ligand simplifies the NMR spectra of the complexes and permits a detailed conformational analysis which is reinforced by an X-ray determination of the dinuclear complex $[(bpy)_2Ru(\mathbf{2c})Ru(bpy)_2](PF_6)_4$, which crystallizes in the monoclinic space group $P2_1/n$ with a = 13.535(6) Å, b = 27.399(8) Å, c = 22.400(8) Å, β = 96.72(3)°, μ = 5.39 cm^{-1}, and Z = 4. Communication of the metal centers through the bridging ligand is examined by electronic absorption and emission spectroscopy and electrochemical analysis. Evidence is presented for limited communication between the two halves of the bridging ligand controlled by the length of the central polymethylene bridge.

Introduction

Over the past decade there has been considerable attention directed toward the study of homodinuclear ruthenium(II) 1,4-diimine complexes with the anticipation of developing an effective photoredox catalyst related to the $Ru(bpy)_3^{2+}$ dication (bpy = 2,2′-bipyridine).[1] In addition, a variety of heterodinuclear analogs have also been examined including the Ru(II)–Os(II) system.[2]

Structurally, these complexes can be divided into two categories.[3] One category would involve binucleating bridging ligands such as 2,2′-bipyrimidine, 2,2′-biimidazole, and 2,3-bis(2′-pyridyl)pyrazine, among others, in which the two metals are held in a rigid and well-defined orientation with respect to one another on opposite sides of the bridging ligand.[4-15] Interactions between the two metal centers are often mediated by the degree to which the bridging ligand facilitates electronic communication through its π-network. The second category of complexes involves two bidentate chelators such as bpy or 1,10-phenanthroline connected by a flexible tether allowing the metal centers considerable latitude in their proximity to one another.[16-19] Oftentimes complexes of this latter type behave much like their independent mononuclear components.

We have recently prepared a series of polyaza cavity-shaped molecules consisting of pyridine and 1,8-naphthyridine rings connected through their α-positions.[20] To control the conformation of these cavities, polymethylene bridges have been incorporated between the β-positions on adjacent rings. This paper will consider polyaza cavities **2** wherein every nonbridgehead

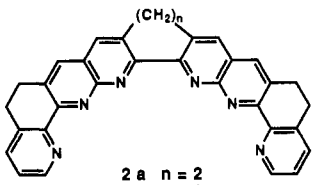

2 a n = 2
b n = 3
c n = 4

position on the interior or bay region of the cavity is an sp^2-hybridized nitrogen. These systems may also be viewed as three 3,3′-bridged derivatives of bpy fused to one another such that they share a common 2,3-bond. These cavities possess three potential bidentate chelating sites: one central site and two equivalent distal sites. The likelihood of coordination is controlled both by the steric accessibility of the site as well as the dihedral angle between the two halves of the bpy moiety as dictated by the 3,3′-bridge.

As a bridging ligand, these polyaza cavities offer an intriguing alternative to the two categories of ligands outlined earlier. The metal centers would both be chelated in the bay region, and their relative orientation would be controlled by the length of the central polymethylene bridge. This paper will discuss the preparation and properties of mononuclear Ru(II) and Os(II) complexes, homodinuclear Ru(II)–Ru(II) complexes, and a heterodinuclear Ru(II)–Os(II) complex of these cavities as depicted in Figure 1.

Experimental Section

Nuclear magnetic resonance spectra were recorded on a Nicolet NT-300 WB spectrometer or a General Electric QE-300 spectrometer at 300 MHz for ^1H NMR and 75 MHz for ^{13}C NMR. Chemical shifts are

(1) (a) Balzani, V.; Scandola, F. *Supramolecular Photochemistry*; Horwood: Chichester: U.K., 1991. (b) Kalyanasundaram, K. *Photochemistry of Polypyridine and Porphyrin Complexes*; Academic: San Diego, CA, 1992.
(2) Hage, R.; Haasnoot, J. G.; Nieuwenhuis, H. A.; Reedijk, J.; De Ridder, D. J. A.; Vos, J. G. *J. Am. Chem. Soc.* **1990**, *112*, 9245.
(3) For an excellent review on bridging ligands see: Steel, P. J. *Coord. Chem. Rev.* **1990**, *106*, 227.
(4) Braunstein, C. H.; Baker, A. D.; Strekas, T. C.; Gafney, H. D. *Inorg. Chem.* **1984**, *23*, 857.
(5) Fuchs, Y.; Lofters, S.; Dieter, T.; Shi, W.; Morgan, R.; Strekas, T. C.; Gafney, H. D.; Baker, A. D. *J. Am. Chem. Soc.* **1987**, *109*, 2691.
(6) Berger, R. M. *Inorg. Chem.* **1990**, *29*, 1920.
(7) Campagna, S.; Denti, G.; De Rosa, G.; Sabatino, L.; Ciano, M.; Balzani, V. *Inorg. Chem.* **1989**, *28*, 2565.
(8) Denti, G.; Campagna, S.; Sabatino, L.; Serroni, S.; Ciano, M.; Balzani, V. *Inorg. Chem.* **1990**, *29*, 4750.
(9) Cooper, J. B.; MacQueen, D. B.; Peterson, J. D.; Wertz, D. W. *Inorg. Chem.* **1990**, *29*, 3701.
(10) Hage, R.; Dijkhuis, A. H. J.; Haasnoot, J. G.; Prins, R.; Reedijk, J.; Buchanan, B. E.; Vos, J. G. *Inorg. Chem.* **1988**, *27*, 2185.
(11) Hage, R.; Haasnoot, J. G.; Reedijk, J.; Wang, R.; Vos, J. G. *Inorg. Chem.* **1991**, *30*, 3263.
(12) Rillema, D. P.; Callahan, R. W.; Mack, K. B. *Inorg. Chem.* **1982**, *21*, 2589.
(13) Rillema, D. P.; Mack, K. B. *Inorg. Chem.* **1982**, *21*, 3849.
(14) Haga, M.; Matsumura-Inoue, T.; Yamabe, S. *Inorg. Chem.* **1987**, *26*, 4148.
(15) Dose, E. V.; Wilson, L. J. *Inorg. Chem.* **1978**, *17*, 2660.
(16) De Cola, L.; Belser, P.; Ebmeyer, F.; Barigelletti, F.; Vögtle, F.; von Zelewsky, A.; Balzani, V. *Inorg. Chem.* **1990**, *29*, 495.
(17) Tinnemans, A. H. A.; Timmer, K.; Reinten, M.; Kraajkamp, J. G.; Alberts, A. H.; van der Linden, J. G. M.; Schmitz, J. E. J.; Saaman, A. A. *Inorg. Chem.* **1981**, *20*, 3698.
(18) Furue, M.; Kinoshita, S.; Kushida, T. *Chem. Lett.* **1987**, 2355.
(19) (a) Shaw, J. R.; Webb, R. T.; Schmehl, R. H. *J. Am. Chem. Soc.* **1990**, *112*, 1117. (b) Ryu, C. K.; Schmehl, R. H. *J. Phys. Chem.* **1989**, *93*, 7961. (c) Schmehl, R. H.; Auerbach, R. A.; Wacholtz, W. F. *J. Phys. Chem.* **1988**, *92*, 6202. (d) Wachiltz, W. F.; Auerbach, R. A.; Schmehl, R. H. *Inorg. Chem.* **1987**, *26*, 2989.
(20) Thummel, R. P.; Hery, C.; Williamson, D.; Lefoulon, F. *J. Am. Chem. Soc.* **1988**, *110*, 7894.

0020-1669/93/1332-1587$04.00/0

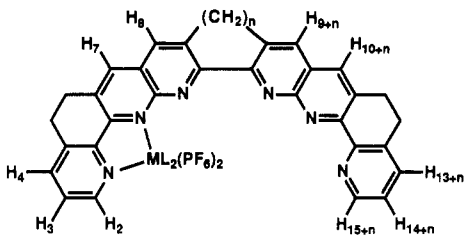

[Ru(**2a**)(bpy)$_2$](PF$_6$)$_2$
[Ru(**2b**)(bpy)$_2$](PF$_6$)$_2$
[Ru(**2c**)(bpy)$_2$](PF$_6$)$_2$
[Ru(**2a**)(bpy-d$_8$)$_2$](PF$_6$)$_2$
[Ru(**2c**)(bpy-d$_8$)$_2$](PF$_6$)$_2$
[Os(**2c**)(bpy-d$_8$)$_2$](PF$_6$)$_2$

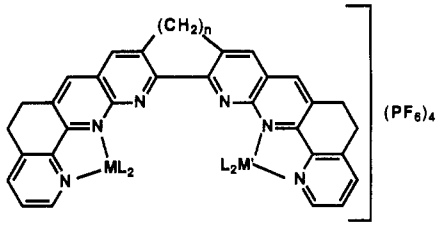

[(bpy)$_2$Ru(**2b**)Ru(bpy)$_2$](PF$_6$)$_4$
[(bpy)$_2$Ru(**2c**)Ru(bpy)$_2$](PF$_6$)$_4$
[(bpy-d$_8$)$_2$Ru(**2c**)Os(bpy-d$_8$)$_2$](PF$_6$)$_4$

Figure 1. Structures of large cavity complexes.

reported in parts per million downfield from Me_4Si or sodium 3-(trimethylsily)propanoate-2,2,3,3-d_4 (in D_2O). Infrared spectra were obtained on a Perkin-Elmer 1330 spectrometer. Electronic spectra were obtained on Perkin-Elmer 330 spectrophotometer. Emission spectra were obtained on a Perkin-Elmer LS-50 luminescence spectrometer using a Hamamatsu R928 HA photomultiplier tube. The tube is sensitive to about 850 nm, and an emission response curve supplied by the manufacturer is deposited with the supplementary material. Cyclic voltammograms were recorded using a BAS CV-27 voltammograph and a Houston Instruments Model 100 X-Y recorder according to a procedure which has been previously described.[21] All solvents were freshly distilled reagent grade, and all melting points are uncorrected.

Mass spectra were obtained on a Hewlett Packard 5933A GC-mass spectrometer. Fast-atom bombardment (FAB) mass spectra of Ru(II) and Os(II) complexes were acquired on a VG 70-SEQ mass spectrometer with EBQQ geometry.[22] Electrospray ionization mass spectra of Ru(II) complexes were performed by Dr. V. Katta at the Rockfeller University, New York, NY. High-resolution mass spectral analyses were performed by Dr. H. Webb at the University of California, Santa Barbara, CA.

Literature procedures were followed for the preparation of the following compounds: 1,2-cyclohexanedione (**3a**),[23] 1,2-cycloheptanedione (**3b**),[24] 1,2-cyclooctanedione (**3c**),[25] 2-amino-5,6-dihydro-1-phenanthridine-3-carboxaldehyde (**4a**),[26] 2-amino-5,6-dihydro-1,10-phenanthroline-3-carboxaldehyde (**4b**),[26] 4-aminopyrimidine-5-carboxaldehyde (**5**),[27] [*cis*-Ru(bpy)$_2$Cl$_2$]·2H$_2$O,[28] and [*cis*-Ru(bpy-d$_8$)$_2$Cl$_2$]·2H$_2$O.[29]

For NMR purposes the ligand numbering scheme starts with the terminal benzo or pyrido ring and assigns the number one to the CH or N adjacent to a bridgehead position on the interior of the cavity. Proceeding away from the cavity, around the perimeter, every non-bridgehead position is numbered sequentially (see Figure 1). For metal complexes, numbering begins closest to the metal of lowest atomic number. Positions identical by symmetry are indicated only by the lowest number.

5,6,9,10,13,14-Hexahydrodibenzo[*b*]quinolino[2,3-*b*:3,2′-*j*][1,10]-phenanthroline (1a). To a refluxing solution of 2-amino-5,6-dihydro-1-phenanthridine-3-carboxaldehyde (**4a**, 0.23 g, 1.02 mmol) and 1,2-cyclohexanedione (**3a**, 0.05 g, 0.45 mmol) in 20 mL of absolute ethanol were added 4 drops of 15% methanolic KOH, and reflux was continued overnight. The precipitate which formed upon cooling was collected by filtration to afford 0.16 g (73%) of **1a**, mp > 300 °C: ^{1}H NMR (300 MHz, $CDCl_3$) δ 8.88 (d, 2H, H_1, $J_{1,2}$ = 7.4 Hz), 7.98 (s, 2H, H_7 or H_8), 7.89 (s, 2H, H_7 or H_8), 7.46 (d of t, 2H, H_2, $J_{2,3}$ = 7.4, $J_{2,4}$ = 1.5 Hz), 7.40 (d of t, 2H, H_3, $J_{3,4}$ = 7.4, $J_{3,1}$ = 1.5 Hz), 7.28 (d, 2H, H_4), 3.27 (s, 4H, H_9), 3.18 (dd, 4H), 3.06 (dd, 4H); IR (KBr) 1610, 1595, 1520, 1460, 1420, 1400, 1020, 780, and 740 cm^{-1}; mass spectrum, *m/e* (rel intensity) 489 (15, M + 1), 488 (44, M), 487 (76), 486 (81), 485 (100), 484 (39), 483 (59), 242 (55); HRMS calcd for $C_{34}H_{24}N_4$ (M − 2) 486.1844, found 486.1778.

6,9,10,11,14,15-Heptahydro-5*H*-cyclohepta[1″,2″:5,6;4″,3:5′,6′]dipyrido[2,3-*b*:2′,3′-*b*′]dibenzo[*h*]quinoline (1b). Following the same procedure described for **1a**, the reaction of **4a** (0.25 g, 1.12 mmol) with 1,2-cycloheptanedione (**3b**, 0.062 g, 0.49 mmol) afforded 0.15 g (61%) of **1b**, mp > 300 °C: ^{1}H NMR (300 MHz, $CDCl_3$) δ 8.82 (d, H_1, 2H, $J_{1,2}$ = 8.5 Hz), 7.94 (s, 2H, H_7 or H_8), 7.93 (s, 2H, H_7 or H_8), 7.38 (overlapping t, 4H, H_2, H_3), 7.26 (d, 2H, H_4, $J_{4,3}$ = 5.5 Hz), 3.18 (dd, 4H), 3.05 (dd, 4H), 2.77 (t, 4H, H_9, $J_{9,10}$ = 6.7 Hz), 2.23 (quintet, 2H, H_{10}); IR (KBr) 1610, 1595, 1525, 1460, 1450, 1415, 1325, 1150, 1140, 775, and 730 cm^{-1}; mass spectrum, *m/e* (rel intensity) 503 (87, M + 1), 502 (M, 100), 501 (81), 500 (84); HRMS calcd for $C_{35}H_{26}N_4$ 502.2157, found 502.2160.

5,6,9,10,11,12,15,16-Octahydrocycloocta[1″,2″:5,6;4″,3″:5′,6′]dipyrido[2,3-*b*:2′,3′-*b*′]dibenzo[*h*]quinoline (1c). Method A. Following the same procedure described for **1a**, the reaction of **4a** (0.224 g, 1.0 mmol) with 1,2-cyclooctanedione (**3c**, 0.064 g, 0.45 mmol) afforded 0.18 g (78%) of **1c**, mp > 300 °C: ^{1}H NMR ($CDCl_3$) δ 8.71 (d, H_1, $J_{1,2}$ = 4.0 Hz), 7.94 (s, 2H, H_7 or H_8), 7.89 (s, 2H, H_7 or H_8), 7.31 (m, 4H, H_2, H_3), 7.20 (m, 2H, H_4), 3.13 (m, 4H, $-CH_2-$), 3.00 (m, 4H, $-CH_2-$), 2.92 (dd, 2H), 2.41 (dd, 2H), 2.19 (t, 2H), 1.62 (m, 2H); IR (KBr) 2940, 1606, 1540, 1474, 1425, 1315, 1265, 1125, 1040, 1034, 940, 788, 748, 735 cm^{-1}; mass spectrum, *m/e* (rel intensity) 518 (10, M + 2), 517 (40, M + 1), 516 (92, M), 488 (93), 487 (100).

Method B. Following the same procedure described for **1a**, the reaction of **6** (70 mg, 0.235 mmol) and α-tetralone (**8**, 90 mg, 0.59 mmol) provided 73 mg (60%) of **1c** having spectral characteristics identical to those described in method A.

5,6,9,10,13,14-Hexahydrodi[1,10]phenanthrolino[2,3-*b*:3′,2′-*j*][1,10]-phenanthroline (2a). Following the same procedure described for **1a**, the reaction of **4b** (0.23 g, 1.02 mmol) with 1,2-cyclohexanedione (**3a**, 0.50 g, 0.45 mmol) afforded 0.139 g (63%) of **2a**, mp > 300 °C: ^{1}H NMR (300 MHz, DMSO-d_6) δ 8.73 (broad s, 2H, H_2), 8.37 (s, 2H, H_7 or H_8), 8.32 (s, 2H, H_7 or H_8), 7.84 (d, 2H, H_4, $J_{4,3}$ = 7.1 Hz), 7.46 (d of d, 2H, H_3), 3.27 (s, 4H, $-CH_2-$), 3.20 (m, 4H, $-CH_2-$), 3.09 (m, 4H, $-CH_2-$); IR (KBr) 2930, 1650, 1635, 1605, 1530, 1520, 1435, 1300, 1150, 1100, 1030, 790 cm^{-1}; mass spectrum, *m/e* (rel intensity) 492 (100, M + 2), 491 (82, M + 1), 489 (67), 488 (74), 487 (74); HRMS calcd for $C_{32}H_{22}N_6$ 488.1749 (M − 2), found 488.1616.

5,6,9,10,11,14,15-Heptahydro-5*H*-cyclohepta[1″,2″:5,6;4″,3″:5′,6′]-dipyrido[2,3-*b*:2′,3′-*b*′]di[1,10]phenanthroline (2b). Following the same procedure described for **1a**, the reaction of **4b** (0.210 g, 0.93 mmol) with 1,2-cycloheptanedione (**3b**, 0.056 g, 0.44 mmol) afforded 0.207 g of material which was chromatographed on alumina eluting with chloroform followed by 98:2 chloroform–ethanol. The first fractions of the mixed eluent gave 0.117 g (53%) of **2b**, mp > 300 °C: ^{1}H NMR (300 MHz, $CDCl_3$) δ 8.80 (d, 2H, H_2, $J_{2,3}$ = 3.7 Hz), 8.08 (s, 2H, H_7 or H_8), 8.02 (s, 2H, H_7 or H_8), 7.63 (d, 2H, H_4, $J_{4,3}$ = 7.5 Hz), 7.32 (dd, 2H, H_3, $J_{3,2}$ = 3.5, $J_{3,4}$ = 4.7 Hz), 3.23 (t, 4H, $-CH_2-$), 3.09 (t, 4H, $-CH_2-$), 2.76 (t, 4H, $-CH_2-$), 2.26 (quintet, 2H, $-CH_2-$); IR (KBr) 2960, 1605, 1560, 1530, 1435, 1235, 1100, 1060, 1035, 790 cm^{-1}; HRMS (*m/e*) calcd for $C_{33}H_{24}N_6$ 504.2062, found 504.2054.

5,6,9,10,11,12,15,16-Octahydrocycloocta[1″,2″:5,6;4″,3″:5′,6′]dipyrido[2,3-*b*:2′,3′-*b*′]di[1,10]phenanthroline (2c). Following the same procedure described for **1a**, the reaction of **4b** (0.230 g, 1.02 mmol) with 1,2-cyclooctanedione (**3c**, 0.066 g, 0.47 mmol) afforded 0.214 g (88%) of **2c**, mp > 300 °C: ^{1}H NMR (300 MHz, DMSO-d_6) δ 8.69 (d, 2H,

(21) Goulle, V.; Thummel, R. P. *Inorg. Chem.* **1990**, *29*, 1767.
(22) Liang, X.; Suwanrumpha, S.; Freas, R. B. *Inorg. Chem.* **1991**, *30*, 652.
(23) Hach, C. C.; Banks, C. V.; Diehl, H. *Organic Syntheses*; Wiley: New York, 1963; Collect. Vol. IV, p 229.
(24) Vanderhear, R. W.; Voter, R. C.; Banks, C. V. *J. Org. Chem.* **1949**, *14*, 836.
(25) Wittig, G.; Krebs, A. *Chem. Ber.* **1961**, *44*, 3760.
(26) Thummel, R. P.; Lefoulon, F.; Williamson, D.; Chavan, M. *Inorg. Chem.* **1986**, *25*, 1675.
(27) Bredereck, H.; Simchen, G.; Traut, H. *Chem. Ber.* **1967**, *100*, 3664.
(28) Sullivan, B. P.; Salmon, D. J.; Meyer, T. J. *Inorg. Chem.* **1978**, *17*, 3334.
(29) Chirayil, S.; Thummel, R. P. *Inorg. Chem.* **1989**, *28*, 812.

H_2, $J_{2,3}$ = 3.7 Hz), 8.39 (s, 2H, H_7 or H_8), 8.42 (s, 2H, H_7 or H_8), 7.83 (d, 2H, H_4, $J_{4,3}$ = 7.3 Hz), 7.45 (dd, 2H, H_3), 3.23 (m, 4H, $-CH_2-$), 3.11 (m, 4H, $-CH_2-$), 2.90 (m, 2H), 2.25 (m, 4H), 1.65 (m, 2H); IR (KBr) 2920, 1660, 1610, 1530, 1440, 1415, 1235, 1100, 900, 800 cm^{-1}; mass spectrum, *m/e* (rel intensity) 518 (100, M), 517 (98), 210 (30), 100 (58), 81 (65).

5,5′-Tetramethylene-6,6′-di[4,5-*b*]pyrimidopyridine (6). Following the same procedure described for **1a**, the reaction of 4-aminopyrimidine-5-carboxaldehyde (**5**, 0.50 g, 4.07 mmol) and 1,2-cyclooctanedione (**3c**, 0.24 g, 1.7 mmol) afforded a yellow precipitate which was collected by filtration to give 0.34 g (64%) of **6**, mp > 300 °C: ^1H NMR (60 MHz, $CDCl_3$) δ 9.58 (s, 2H, H_2 or H_4), 9.55 (s, 2H, H_2 or H_4), 8.28 (s, 2H, H_5), 3.11 (dd, 2H), 2.45 (dd, 2H), 2.34 (t, 2H), 1.73 (m, 2H), 1.66 (broad s, H_2O); IR (KBr) 1600, 1580, 1540, 1450, 1430, 1360, 1030, 815 cm^{-1}; mass spectrum, *m/e* (rel intensity) 315 (10, M + 1), 314 (44, M), 313 (9), 287 (11), 286 (56), 285 (100).

5,5′-Tetramethylene-6,6′-bis(2-aminopyridine-3-carboxaldehyde) (7). A solution of **6** (0.18 g, 0.57 mmol) in 150 mL of 1 N HCl was refluxed for 4 h. After cooling, neutralization with NH_4OH produced 0.16 g (95%) of **7** as a yellow precipitate, mp > 300 °C: ^1H NMR (300 MHz, $CDCl_3$) δ 9.94 (s, CHO), 7.75 (s, 2H, H_4), 6.74 (broad s, NH_2), 2.72 (dd, 2H), 2.26 (m, 2H), 2.12 (t, 2H), 1.64 (broad s, H_2O), 1.51 (m, 2H); IR (KBr) 1670, 1660, 1620, 1585, 1545, 1450, 1290, 1185, 1135, 745 cm^{-1}; mass spectrum, *m/e* (rel intensity) 297 (20, M + 1), 296 (100, M), 268 (74), 267 (63), 212 (22), 211 (46).

General Procedure for Metal Complexes. A mixture of the ligand and [*cis*-$Ru(bpy)_2Cl_2]\cdot 2H_2O$ was refluxed under nitrogen overnight. After cooling, a solution of 2 equiv of NH_4PF_6 in 5 mL of H_2O was added to precipitate the complex, which was collected, dried, and purified.

[Ru(2a)(bpy)$_2$](PF$_6$)$_2$. The reaction of **2a** (20 mg, 0.04 mmol) with [*cis*-$Ru(bpy)_2Cl_2]\cdot 2H_2O$ (20.4 mg, 0.04 mmol) provided material which was chromatographed on alumina eluting with 1:1 toluene–acetonitrile to afford 30.4 mg (63%) of the complex, which was recrystallized from the same solvent mixture: ^1H NMR (300 MHz, CD_3CN) δ 10.55 (d, 1H, J = 8.2 Hz), 9.16 (d, 1H, J = 8.1 Hz), 8.96 (d, 1H, J = 4.8 Hz), 8.31–7.14 (m, 20 H), 7.10 (d, 1H, J = 5.6 Hz), 6.77 (t, 1H, J = 6.5 Hz), 6.58 (t, 1H, J = 6.5 Hz), 3.5–2.9 (m, 12H); ^{13}C NMR (CD_3CN) δ 153.4, 153.0, 152.1, 151.3, 150.7, 139.3, 139.1, 138.8, 138.4, 137.7, 136.1, 135.9, 135.6, 135.3, 129.6, 129.5, 129.5, 129.3, 128.8, 127.5, 126.7, 126.6, 125.5, 125.4, 29.0, 28.8, 28.7, 27.7; FAB MS *m/e* 1049 [(Ru(**2a**)(bpy)$_2$]PF_6^+, 68), 904 ([Ru(**2a**)(bpy)$_2$]$^+$, 100), 747 ([Ru(**2a**)bpy]$^+$, 53), 592 ([Ru(**2a**)]$^+$, 55), 452 ([Ru(**2a**)(bpy)$_2$]$^{2+}$, 79).

[Ru(2b)(bpy)$_2$](PF$_6$)$_2$. The reaction of **2b** (50.4 mg, 0.10 mmol) with [*cis*-$Ru(bpy)_2Cl_2]\cdot 2H_2O$ (49.3 mg, 0.095 mmol) gave 80 mg of a red solid, which was chromatographed on alumina eluting with 1:1 toluene–acetonitrile to afford 52 mg (45%) of the complex: ^1H NMR (300 MHz, CD_3CN) δ 8.6–7.00 (m, 26 H), 3.6–3.0 (12 H), 2H hidden by the H_2O peak in CD_3CN; FAB MS, *m/e* 1210 ([Ru(**2b**)(bpy)$_2$](PF$_6$)$_2^+$, 6), 1064 ([Ru(**2b**)(bpy)$_2$]PF_6^+, 75), 919 ([Ru(**2b**)(bpy)$_2$]$^+$, 100), 762 ([Ru(**2b**)-bpy]$^+$, 43), 607 ([Ru(**2b**)]$^+$, 44), 459.5 ([Ru(**2b**)(bpy)$_2$]$^{2+}$, 32).

[Ru(2c)(bpy)$_2$](PF$_6$)$_2$. The reaction of **2c** (32 mg, 0.10 mmol) with [*cis*-$Ru(bpy)_2Cl_2]\cdot 2H_2O$ (42 mg, 0.08 mmol) gave a red solid, which was chromatographed on alumina eluting with 1:1 toluene–acetonitrile to afford 42 mg (42%) of the complex: ^1H NMR (300 MHz, CD_3CN) δ 9.40–5.80 (26 H), 3.6–2.8 (12H), 2.2 (4H); FAB MS *m/e* 1077 ([Ru-(**2c**)(bpy)$_2$]PF_6^+, 77), 933 ([Ru(**2c**)(bpy)$_2$]$^+$, 100), 775 ([Ru(**2c**)bpy]$^+$, 75), 620 ([Ru(**2c**)]$^+$, 91), 466.5 ([Ru(**2c**)(bpy)$_2$]$^{2+}$, 81).

[Ru(2a)(bpy-*d*$_8$)$_2$](PF$_6$)$_2$. The reaction of **2a** (50 mg, 0.10 mmol) with [*cis*-$Ru(bpy\text{-}d_8)_2Cl_2]\cdot 2H_2O$ (55 mg, 0.103 mmol) gave a precipitate, which was chromatographed on alumina eluting with 1:1 acetonitrile–toluene to afford 44 mg (36%) of the complex: ^1H NMR (300 MHz, CD_3CN) δ 8.97 (dd, H_{17}, $J_{16,17}$ = 4.8 Hz, $J_{15,17}$ = 1.2 Hz), 8.34 (s, H_7, H_8, H_{11} or H_{12}), 8.24 (s, H_7, H_8, H_{11} or H_{12}), 8.13 (s, H_7, H_8, H_{11} or H_{12}), 8.04 (s, H_7, H_8, H_{11} or H_{12}), 7.92 (d, H_{15}, $J_{15,16}$ = 7.4 Hz), 7.88 (d, H_4, $J_{3,4}$ = 8.0 Hz), 7.73 (d, H_2, $J_{2,3}$ = 5.0 Hz), 7.57 (dd, H_{16}), 7.39 (dd, H_3), 3.25–2.95 (12 H).

[Ru(2c)(bpy-*d*$_8$)$_2$](PF$_6$)$_2$. The reaction of **2c** (0.225 g, 0.433 mmol) with [*cis*-$Ru(bpy\text{-}d_8)_2Cl_2]\cdot 2H_2O$ (0.186 g, 0.346 mmol) gave a precipitate which was chromatographed on alumina eluting with 1:1 acetonitrile–toluene to afford 0.382 g (91%) of the complex, whose ^1H NMR shows two sets of peaks in a 3:2 ratio for the two possible diastereomers: ^1H NMR (300 MHz, CD_3CN) δ 8.91 (d, J = 4.3 Hz), 8.66 (d, J = 4.5 Hz), 8.41 (s), 8.35 (s), 8.29 (s), 8.25 (s), 8.21 (s), 8.14 (s), 7.92 (d, J = 7.8 Hz), 7.87 (m), 7.64 (d, J = 5.3 Hz), 7.55 (dd, J = 4.8, 7.6 Hz), 7.48 (m), 7.33 (m), 3.48–3.53 (m), 3.39–3.17 (m), 2.98–2.83 (m). Two successive recrystallizations from toluene–acetonitrile allowed the isolation of the minor isomer: ^1H NMR (300 MHz, CD_3CN) δ 8.66 (dd, H_{19}, $J_{18,19}$ = 4.8 Hz, $J_{17,19}$ = 0.8 Hz), 8.36 (s, H_7, H_8, H_{13} or H_{14}), 8.26 (s, H_7, H_8, H_{13} or H_{14}), 8.25 (s, H_7, H_8, H_{13} or H_{14}), 8.18 (s, H_7, H_8, H_{13} or H_{14}), 7.88 (d, H_4, $J_{3,4}$ = 7.6 Hz), 7.78 (d, H_{17}, $J_{17,18}$ = 7.4 Hz), 7.47 (d, H_2, $J_{2,3}$ = 5.2 Hz), 7.41 (dd, H_{18}), 7.33 (dd, H_3), 3.47 (m, 2 H), 3.38 (m, 2 H), 3.30 (m, 2 H), 3.21 (m, 2 H), 2.90 (m, 2 H), 6H hidden behind the peak for H_2O in CD_3CN.

[(bpy)$_2$Ru(2b)Ru(bpy)$_2$](PF$_6$)$_4$. The reaction of **2b** (36 mg, 0.07 mmol) with [*cis*-$Ru(bpy)_2Cl_2]\cdot 2H_2O$ (91 mg, 0.18 mmol) gave a red solid, which was chromatographed on alumina eluting with 1:1 toluene–acetonitrile mixture to afford 74 mg (55%) of the dinuclear complex: ^1H NMR (300 MHz, CD_3CN) δ 8.70–4.70 (42 H) 3.8–3.25 (10H), 2.8–2.6 (2H), 1.8–1.7 (2H); FAB MS *m/e* 1769 ([(bpy)$_2$Ru(**2b**)Ru(bpy)$_2$[(PF$_6$)$_3^+$, 39), 1621 ([(bpy)$_2$Ru(**2b**)Ru(bpy)$_2$](PF$_6$)$_2^+$, 95), 1477 ([(bpy)$_2$Ru(**2b**)-Ru(bpy)$_2$](PF$_6$)$^+$, 76), 1331 ([(bpy)$_2$Ru(**2b**)Ru(bpy)$_2$]$^+$, 25), 1172 ([(bpy)$_2$Ru(**2b**)Ru(bpy)]$^+$, 41), 1018 ([(bpy)$_2$Ru(**2b**)Ru]$^+$, 54), 739 ([(bpy)$_2$Ru(**2b**)Ru(bpy)$_2$](PF$_6$)$^{2+}$, 100), 607 ([Ru(**2b**)]$^+$, 85).

[(bpy)$_2$Ru(2c)Ru(bpy)$_2$](PF$_6$)$_4$. The reaction of **2c** (26 mg, 0.05 mmol) with [*cis*-$Ru(bpy)_2Cl_2]\cdot 2H_2O$ (65 mg, 0.13 mmol) gave a red solid, which was chromatographed on alumina eluting with acetonitrile to afford 50 mg (52%) of the dinuclear complex which was recrystallized from acetonitrile–toluene: ^1H NMR (300 MHz, CD_3CN) δ 8.80–5.0 (m, 42 H), 3.8–3.3 (10 H), 2.9–2.6 (4H), 1.75 (m, 2H); FAB MS, *m/e* 1780 ([(bpy)$_2$Ru(**2c**)Ru(bpy)$_2$](PF$_6$)$_3^+$, 100), 1636 ([(bpy)$_2$Ru(**2c**)Ru(bpy)$_2$]-(PF$_6$)$_2^+$, 94), 1491 ([(bpy)$_2$Ru(**2c**)Ru(bpy)$_2$] (PF$_6$)$^+$, 31), 1187 ([(bpy)$_2$-Ru(**2c**)Ru(bpy)]$^+$, 41), 1030 ([(bpy)$_2$Ru(**2c**)Ru]$^+$, 62), 871 ([(bpy)-Ru(**2c**)]$^+$, 57), 775 ([Ru(**2c**)bpy]$^+$, 85), 618 ([Ru(**2c**)]$^+$, 87).

Dichlorobis(2,2′-bipyridine-*d*$_8$)osmium(III) Chloride.[30] A solution of potassium hexachloroosmiate (0.25 g, 0.52 mmol) and 2,2′-bipyridine-d_8 (0.17 g, 1.04 mmol) in dimethylformamide (6 mL) was heated to reflux. After 15 min, KCl began to separate. After 1 h, the solution was cooled, the KCl filtered, and methanol added. Upon addition of ether, 0.206 g (63%) of [Os(bpy-d_8)$_2$Cl$_2$]Cl separated as crystals, which were filtered off and washed with ether.

Dichlorobis(2,2′-bipyridine-*d*$_8$)osmium(II).[30] To a cold solution of [Os(bpy-d_8)$_2$Cl$_2$]Cl (0.206 g, 0.33 mmol) in dimethylformamide (5 mL) and methanol (2 mL) was slowly added a dilute solution of sodium dithionite in water. Upon cooling of the solution overnight to 0 °C, 0.13 g (65%) of Os(bpy-d_8)$_2$Cl$_2\cdot H_2O$ was obtained as a dark purple solid, which was filtered off and dried.

[Os(2c)(bpy-*d*$_8$)$_2$]Cl$_2$. A mixture of **2c** (90 mg, 0.173 mmol) and [Os-(bpy-d_8)$_2$Cl$_2$]$\cdot H_2O$ (100 mg, 0.16 mmol) in 25 mL of 1:1 ethanol–water was refluxed for 48 h. The red solid obtained upon solvent evaporation was chromatographed on alumina eluting with 96:4 acetonitrile–methanol to afford 118 mg (65%) of a violet crystalline solid, which gave an ^1H NMR showing two sets of peaks in a 4:3 ratio corresponding to the two possible diastereomers: 300 MHz, CD_3CN, δ 9.02 (dd, 1H, J = 4.2, 1.2 Hz), 8.79 (dd, 1H, J = 4.2, 0.8 Hz), 8.35 (s, 1H), 8.32 (s, 1H), 8.28 (s, 1H), 8.26 (s, 1H), 8.23 (s, 1H), 8.18 (s, 1H), 8.16 (s, 1H), 8.12 (s, 1H), 8.01 (d, 2H, J = 7.6 Hz), 7.59 (m, 7H), 7.21 (m, 3H), 3.26–3.15 (m, $-CH_2-$), 3.00–2.8 (m, $-CH_2-$); FAB MS, *m/e* 1037 ([Os(bpy-d_8)$_2$(**2c**)]$^+$, 100), 516 (**2c**$^+$, 64).

[Os(2c)(bpy-*d*$_8$)$_2$](PF$_6$)$_2$. A mixture of **2c** (90 mg, 0.17 mmol) and [Os(bpy-d_8)$_2$Cl$_2$]$\cdot H_2O$ (105 mg, 0.17 mmol) in 10 mL of 1:1 ethanol–water was refluxed for 40 h. The reaction mixture was cooled and filtered. The filtrate was treated with NH_4PF_6, and the violet solid obtained by evaporation of the solvent was chromatographed on alumina eluting with 1:1 acetonitrile–toluene to afford 121 mg (53%) of the complex, whose ^1H NMR shows two sets of peaks in a 7:3 ratio corresponding to the two possible diastereomers: ^1H NMR (300 MHz, CD_3CN) δ 8.91 (dd, 1H, J = 4.5, 1.3 Hz), 8.65 (dd, J = 4.6, 1.3 Hz), 8.27 (s), 8.24 (s), 8.21 (s), 8.19 (s), 8.15 (s), 8.13 (s), 8.09 (s), 7.86 (dd, J = 7.6, 0.9 Hz), 7.79 (dd, J = 7.5, 0.9 Hz), 7.63 (m), 7.50 (dd, J = 7.7, 4.7 Hz), 7.41 (dd, J = 8.1, 3.9 Hz), 7.22 (m), 7.17 (dd, J = 7.8, 1.9 Hz), 3.30–3.05 (m, 12H, $-CH_2-$), 3.0–2.8 (m, 4H, $-CH_2-$); FAB MS, *m/e* 1329 ([Os(bpy-d_8)$_2$-(**2c**)](PF$_6$)$_2^+$, 15), 1184 ([Os(bpy-d_8)$_2$(**2c**)](PF$_6$)$^+$, 62), 1037 ([Os(bpy-d_8)$_2$(**2c**)]$^+$, 100), 871 ([Os(bpy-d_8)(**2c**)]$^+$, 19), 709 ([Os(**2c**)]$^+$, 27), 519 (**2c**$^+$, 76).

[(bpy-*d*$_8$)$_2$Os(2c)Ru(bpy-*d*$_8$)$_2$](PF$_6$)$_4$. A solution of [Os(**2c**)(bpy-d_8)$_2$]-Cl_2 (90 mg, 0.08 mmol) and [Ru(bpy-d_8)Cl$_2$]$\cdot 2H_2O$ (65 mg, 0.12 mmol) in 25 mL of 1:1 EtOH–H_2O was refluxed overnight. The solution was cooled and filtered, and NH_4PF_6 was added to the filtrate. The crude solid obtained upon solvent evaporation was chromatographed on alumina

(30) Buckingham, D. A.; Dwyer, F. P.; Goodwin, H. A.; Sargeson, A. M. *Aust. J. Chem.* **1964**, *17*, 325.

Table I. Crystallographic Data for $[(bpy)_2Ru(\mathbf{2c})Ru(bpy)_2](PF_6)_4$

chem formula	$C_{74}H_{58}N_{14}Ru_2^{4+}(PF_6^-)_4 \cdot {}^1/_2C_2H_3N \cdot {}^1/_2C_7H_8$
fw	1992.09
cell constants	a = 13.535(6) Å
	b = 27.399(8) Å
	c = 22.400(8) Å
	β = 96.72(3)°
V	8250 Å^3
space group	$P2_1/n$ (monoclinic)
formula units per cell	Z = 4
density	ρ = 1.60 g cm^{-3}
abs coeff	μ = 5.39 cm^{-1}
radiation (Mo Kα)	λ = 0.710 73 Å
R^a	0.064
$R_w{}^a$	0.053

^{a} $R = \sum||F_o| - |F_c||/\sum|F_o|$, $R_w = [\sum w(|F_o| - |F_c|)^2/\sum w|F_o|^2]^{1/2}$, with $w = \sigma(F)^{-2}$.

eluting with 3:7 toluene–acetonitrile to afford 65 mg (40%) of the heterodinuclear complex: ^{1}H NMR (300 MHz, CD_3CN) δ 8.53 (s, 1H), 8.35 (s, 1H), 8.22 (s, 1H), 8.13 (s, 1H), 7.91 (d, 1H, J = 7.9 Hz), 7.63 (t, 2H), 7.46–7.31 (m, 2H), 7.17 (dd, 1H), 3.7–3.3 (m, 8H), 2.8–2.6 (m, 2H), 1.8 (m, 2H), 1.3 (m, 2H), 1.1 (m, 2H); electrospray ionization MS m/e 878 ($(M - 2PF_6)^{2+}$), 537 ($(M - 3PF_6)^{3+}$), 489 ($(537 - HPF_6)^{3+}$), 427, 367 ($(M - 4PF_6)^{4+}$), 341 ($[Os(bpy\text{-}d_8)_3]^{2+}$).

X-ray Determination of $[(bpy)_2Ru(2c)Ru(bpy)_2](PF_6)_4$. A black-cherry colored irregular slab having approximate dimensions 0.40 × 0.30 × 0.25 mm was carved from a large plate and mounted in a random orientation on a Nicolet R3m/V automatic diffractometer. The radiation used was Mo Kα monochromatized by a highly ordered graphite crystal. Data collection was performed at 23 °C. Final cell constants, as well as other information pertinent to data collection and refinement, are listed in Table I. The Laue symmetry was determined to be $2/m$, and from the systematic absences noted the space group was shown unambiguously to be $P2_1/n$. Intensities were measured using the Ω scan technique, with the scan rate depending on the count obtained in rapid prescans of each reflection. Two standard reflections were monitored after every 2 h or every 100 data collected, and these showed no significant variation. In the reduction of the data, Lorentz and polarization corrections were applied; however, no correction for absorption was made due to the small absorption coefficient.

The structure was solved by use of the SHELXTL Patterson interpretation program, which revealed the positions of the two Ru atoms in the cation. The remaining non-hydrogen atoms were located in subsequent difference Fourier syntheses. Hydrogens were added at ideal calculated positions and constrained to riding motion, with a single variable isotropic thermal parameter. It was very quickly found that all four anions are disordered over two slightly different positions, and due to the complexity this disorder entails, it was decided to treat the eight independent units as ideal rigid bodies on the basis of the geometry noted in previous refinements of PF_6^-. The distances and angles for the P1 unit are listed in the supplementary tables, with the other seven units being identical. Occupancy factors for each anionic unit were determined by allowing them to vary while keeping the fluorine isotropic temperature factors nearly the same, resulting in values of 0.60, 0.60, 0.70, 0.65 for the P(1), P(2), P(3), and P(4) units, respectively, with corresponding values of 0.40, 0.40, 0.30, and 0.35 for P(1′), P(2′), P(3′), and P(4′). In the final cycles of refinement, the occupancy factors were fixed at these values. Anisotropic thermal parameters were used for each of the major component fluorines; however, the minor component fluorines had to be held isotropic due to the close proximity of other atoms and/or the lower occupancies involved. The phosphorous atoms also had to be held at fixed isotropic values due to the high correlations noted between the disordered pairs.

In addition to the cation and anions, molecules of solvation were found in partially occupied sites. There is one molecule of acetonitrile, refined with 50% population factors on the basis of an estimate of isotropic thermal motion, and one molecule of toluene which lies quite close to an inversion center and must therefore be substantially disordered over two interlocking sites. The toluene was refined as a rigid body, assuming 50% occupancy at each site, which resulted in acceptable thermal parameters. No attempt was made to include hydrogen atoms on the solvent molecules.

Due to the enormous number of independent variables involved in this refinement, the least squares had to be performed on two separate blocks comprised of 600 variables for all Ru, P, and F atoms as well as N(1) through C(40), followed by 459 variables for the bipyridyls and solvent molecules. After all shift/esd ratios in the cation were less than 0.3; convergence was reached at the agreement factors listed in Table I. No unusually high correlations were noted between any of the variables in the last cycle of full-matrix least-squares refinement, and the final difference density map showed no peak greater than 0.6 e/Å^3. The quality of the structural analysis was to some extent limited by the small size of the crystal and the disorder of the PF_6^- anions over multiple positions. All calculations were made using Nicolet's SHELXTL PLUS series of crystallographic programs.[31]

Synthesis of the Ligands and Complexes

The key reaction employed in the synthesis of the ligand systems is the Friedländer condensation wherein an aromatic *ortho*-aminoaldehyde condenses with a ketone to provide a quinoline or 1,8-naphthyridine nucleus.[32] The aminoaldehydes required for the preparation of **1** and **2** were **4a,b** which have been described previously.[26] Treatment of the cyclic 1,2-diketones **3a–c** with **4** resulted in a 2-fold condensation leading directly to the desired cavities in yields of 61–88%. These compounds were sparingly soluble in chloroform such than ^{1}H NMR analysis was possible but useful ^{13}C spectra could not be obtained.

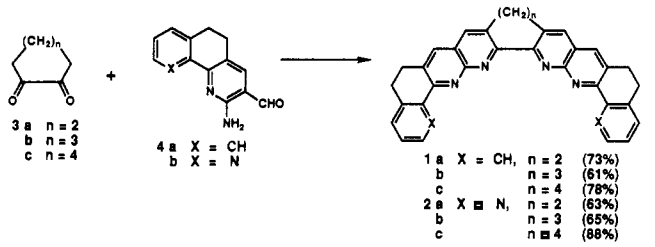

An alternative approach was also investigated for the preparation of these cavities. Once again, the key step was a double Friedländer condensation to form the two 1,8-naphthyridine moieties, but in this case, the distal tetrahydroquinoline portion is introduced as the ketone partner. A 2-equiv amount of 4-amino-5-pyrimidinecarboxaldehyde (**5**)[27] was condensed with 1,2-

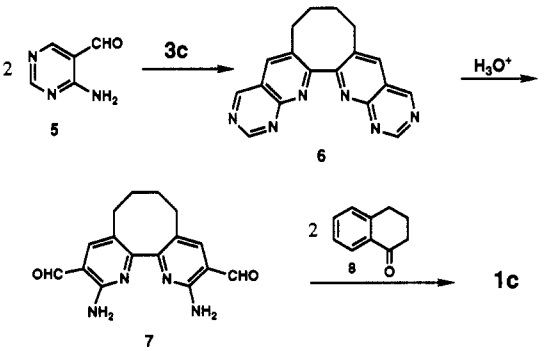

cyclooctanedione (**3c**) to provide **6**, which was hydrolyzed to the tetramethylene-bridged 2,2′-bipyridine diaminodialdehyde **7**. Further condensation of this species with **8** afforded a 60% yield of **1c**. Since the route involving **4** proceeded in somewhat better yield and was more general, this latter approach was not utilized further.

When **2a** was treated with 1 equiv of $[cis\text{-}Ru(bpy)_2Cl_2]\cdot 2H_2O$, a 1:1 complex was formed. The question arises as to whether the $Ru(bpy)_2^{2+}$ is chelated at the central or distal bipyridine moiety. The symmetries of the two complexes resulting from either mode of complexation are different, and a careful analysis of the NMR spectra provides an answer to this question. The ^{1}H NMR (Figure

(31) Sheldrick, G. M. In *Crystallographic Computing* 3; Sheldrick, G. M., Kruger, C., Goddard, R., Eds.; Oxford University Press: Oxford, U.K., 1985; pp 175–189.
(32) Thummel, R. P. *Synlett* **1992**, 1.

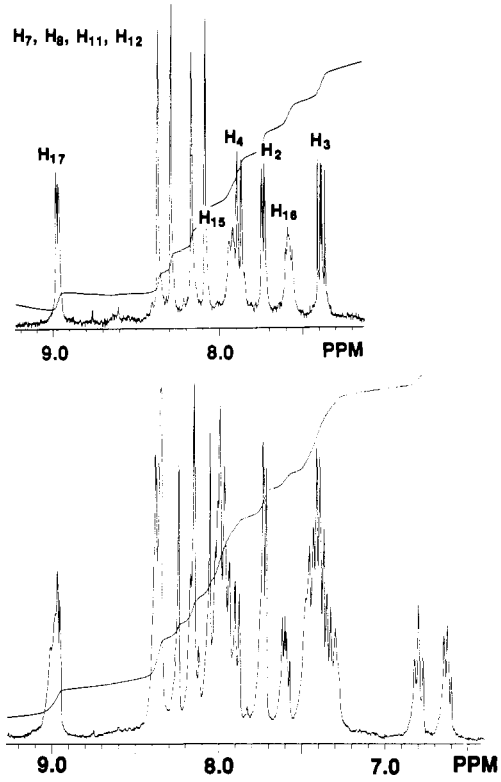

Figure 2. Downfield region of the ^1H NMR spectra of $[Ru(\mathbf{2a})(bpy)_2](PF_6)_2$ (bottom) and $[Ru(\mathbf{2a})(bpy\text{-}d_8)_2](PF_6)_2$ (top) recorded at 300 MHz in CD_3CN. Proton numbering scheme is given in Figure 1.

2, bottom) exhibits 26 signals in the aromatic region including four distinct singlets for the naphthyridine protons of **2a**. The ^{13}C NMR of this complex shows at least four signals in the aliphatic region, ruling out binding of the $Ru(bpy)_2^{2+}$ to the central bpy, which would give a complex with only three nonequivalent methylene carbons.

We examined the likelihood of $Ru(bpy)_2^{2+}$ binding to the central bpy by treating **1a** with $[cis\text{-}Ru(bpy)_2Cl_2]\cdot 2H_2O$. The ligand **1a** no longer possesses a distal bpy binding site. No reaction was observed, indicating that $Ru(bpy)_2^{2+}$ is too sterically demanding to chelate at the central bpy. For **2b,c**, coordination of $Ru(bpy)_2^{2+}$ at the central site is even more unlikely due to the less favorable dihedral angle about the central bond. Treatment of the ligands **2b,c** with 1 equiv of $[cis\text{-}Ru(bpy)_2Cl_2]\cdot 2H_2O$ followed by anion interchange with hexafluorophosphate led to the mononuclear complexes $[Ru(\mathbf{2b,c})(bpy)_2](PF_6)_2$ with the metal bound at a distal site.

We have recently developed a useful technique which facilitates more detailed analysis of the ^1H NMR spectra of unsymmetrical complexes such as $Ru(bpy)_2L^{2+}$. When bpy-d_8 is substituted for bpy in the reagent $[cis\text{-}Ru(bpy)_2Cl_2]\cdot 2H_2O$, the resulting complexes exhibit only ^1H signals from the ligand L.[29] Figure 2 compares the downfield regions of the ^1H NMR spectra of $[Ru(\mathbf{2a})(bpy)_2](PF_6)_2$ and $[Ru(\mathbf{2a})(bpy\text{-}d_8)_2](PF_6)_2$. Whereas relatively little useful structural information can be garnered from the lower spectrum, the top one allows for complete assignment of the 10 nonequivalent aromatic protons of **2a** in the complex with the exception of the four naphthyridine singlets, which nevertheless were all clearly resolved. It is worthwhile to note certain differences in the two sets of terminal pyridyl protons. For H_2–H_4, which are bound to the coordinated pyridyl ring, the signals are much sharper, indicating a more rigid, well-defined environment. This contrasts the somewhat broader signals for H_{15}–H_{17}, which are part of the unbound pyridyl ring and thereby experience more conformational mobility on the NMR time scale due to rotation about the bond joining this ring to the adjacent 1,8-naphthyridine subunit.

The two upfield apparent triplets (actually doublets of doublets) in the lower spectrum of Figure 2 are assigned to H_3 and H_4 on the bpy pyridyl ring bound trans to N_1. Inspection of a molecular model indicates that these protons point into the molecular cavity where they are shielded by the proximate naphthyridine ring on the unbound half of **2a**.

The same technique of replacing bpy with bpy-d_8 was employed in the preparation of the osmium reagent. Complexation of 1 equiv of $[Os(bpy\text{-}d_8)_2Cl_2]$ with **2c** and metathesis to the hexafluorophosphate salt afforded the corresponding mononuclear complex $[Os(\mathbf{2c})(bpy\text{-}d_8)_2](PF_6)_2$.

When **2a** was treated with 2.5 equiv of $[cis\text{-}Ru(bpy)_2Cl_2]\cdot 2H_2O$, only the mononuclear complex was obtained. It appears that the cavity of this ligand is too small for the introduction of a second $Ru(bpy)_2^{2+}$ unit. However, the binuclear complexes $[(bpy)_2Ru(\mathbf{2b,c})Ru(bpy)_2](PF_6)_4$ were prepared by treatment of the ligands **2b,c** with 2.5 equiv of $[cis\text{-}Ru(bpy)_2Cl_2]\cdot 2H_2O$ and precipitation of the complex as its hexafluorophosphate salt. The heterodinuclear complex $[(bpy\text{-}d_8)_2Ru(\mathbf{2c})Os(bpy\text{-}d_8)_2](PF_6)_4$ was prepared by treatment of $[Os(\mathbf{2c})(bpy\text{-}d_8)_2]Cl_2$ with 1.5 equiv of $[cis\text{-}Ru(bpy\text{-}d_8)_2Cl_2]\cdot 2H_2O$ and precipitation with hexafluorophosphate. There was no evidence for any Ru–Os transmetalation in the formation of this complex.

Conformational Properties

In earlier work we have prepared and studied the conformational properties of a series of Ru(II) complexes with 3,3′-polymethylene-bridged derivatives of bpy.[33] The dihedral angle between the two halves of the bpy varies as a function of the length of the polymethylene bridge. At room temperature, we observed by NMR that, for the dimethylene-bridged system ($n = 2$), inversion between the conformational enantiomers A and B was rapid for

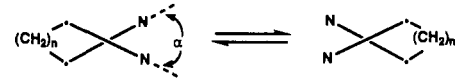

A B

both the free and complexed ligand. If we assume similar mobility for the two dimethylene bridges of **1** and **2**, then it will be the length of the central bridge which will be the most critical in dictating the properties of the ligand.

The tetramethylene-bridged bpy derivative ($n = 4$) is found to be conformationally rigid on the NMR time scale and thus can give rise to discrete conformational enantiomers A and B. For the complex $Ru(bpy)_2L^{2+}$, where L is the 3,3′-tetramethylene-bridged bpy, we have observed that coordination is diastereoselective such that only the [Δ,*d*; Λ,*l*] isomer is obtained. The complex $[Ru(\mathbf{2c})(bpy)_2]^{2+}$ embodies a similar situation except that the tetramethylene-bridged bpy portion of the molecule is not coordinated to Ru(II). Inversion about this central bridge would nevertheless still lead to two diastereomers, [Δ,*d*; Λ,*l*] and [Δ,*l*; Λ,*d*], and if this process is slow on the NMR time scale, one might see distinct signals from both conformations. This is indeed the case as is illustrated in Figure 3. The upper spectrum depicts the ^1H aromatic region for $[Ru(\mathbf{2c})(bpy\text{-}d_8)_2](PF_6)_2$ wherein all the auxilliary bpy resonances have been eliminated by deuterium substitution. The resonance for H_2 of the distal bound pyridyl ring of **2c** appears as two doublets at 8.92 and 8.67 ppm in a 3:2 ratio. These signals arise from the two diastereomeric forms of the equilibrated complex. One can also note two sets of four singlets, at 8.14–8.42 ppm, for the naphthyridine protons of **2c** in approximately the same 3:2 ratio.

The corresponding osmium complex $[Os(\mathbf{2c})(bpy\text{-}d_8)_2](PF_6)_2$ gave an NMR spectrum very similar to that shown in the top of Figure 3. Two diastereomeric forms are again found with H_2 appearing as two sets of doublets at 8.91 and 8.65 ppm in the

(33) Thummel, R. P.; Lefoulon, F.; Korp, J. D. *Inorg. Chem.* **1987**, *26*, 2370.

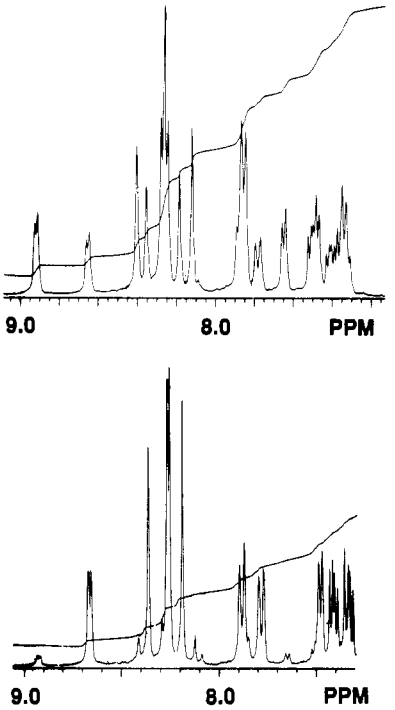

Figure 3. Downfield region of the ^{1}H NMR spectra of [Ru(**2c**)(bpy-d_8)$_2$](PF$_6$)$_2$ recorded at 300 MHz in CD_3CN: Equilibrated mixture of diastereomers (top) and purified minor diastereomer after a small degree of equilibration (bottom).

same approximate 3:2 ratio. The close similarity of their NMR spectra leads to the conclusion that the geometries of the Ru(II) and Os(II) complexes of **2c** are nearly identical.

Successive recrystallization of [Ru(**2c**)(bpy-d_8)$_2$](PF$_6$)$_2$ from acetonitrile/toluene affords the minor component as a single pure diastereomer, and the aromatic region of its ^{1}H NMR spectrum is illustrated in the lower half of Figure 3 after a small degree of equilibration has occurred. With increased time, a second set of peaks corresponding to the other diastereomer appeared. A kinetic experiment was carried out monitoring the two downfield doublets with respect to time at three temperatures (25, 30, and 35 °C). Above 35 °C the equilibration was too rapid to allow an accurate NMR determination. When the values of ln k_A and ln k_B are plotted vs $1/T$, the activation energies for the A,B interconversion could be calculated. The free energies for the two diastereomers differ only by about 1 kcal/mol, but the barrier separating them is approximately 35 ± 5 kcal/mol.[34] We have previously estimated the inversion barrier for 3,3′-tetramethylene-2,2′-bi[1,8]naphthyridine to be 19 kcal/mol.[35] We expect the barrier for the somewhat bulkier free ligand **2c** to be higher. Introduction of a Ru(bpy-d_8)$_2^{2+}$ moiety into the cavity should considerably increase the inversion barrier so that the measured value seems quite reasonable.

The introduction of a second Ru(bpy)$_2^{2+}$ into the cavity of [Ru(**2b,c**)(bpy)$_2$](PF$_6$)$_2$ significantly increases the steric congestion and limits conformational mobility. Inversion about the central bond of **2c** in the dinuclear complex is no longer possible. A single-crystal X-ray analysis of [(bpy)$_2$Ru(**2c**)Ru(bpy)$_2$](PF$_6$)$_4$ was carried out. An ORTEP drawing of the cation is shown in Figure 4, the data collection and processing parameters are listed in Table I, the atomic coordinates and isotropic displacement parameters are listed in Table II, and selected bond lengths, angles, and torsion angles are listed in Table III.

One sees that the bridging ligand has adopted a partially helical conformation and the two Ru(bpy)$_2^{2+}$ moieties are held in close

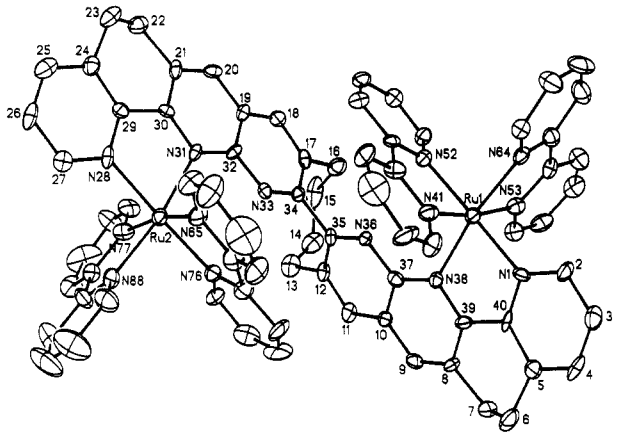

Figure 4. View of the [(bpy)$_2$Ru(**2c**)Ru(bpy)$_2$]$^{4+}$ cation, with labeling of key atoms. The thermal ellipsoids are 20% equiprobability envelopes, and hydrogens have been omitted for clarity.

proximity. The Ru(1)–Ru(2) distance is 8.12 Å, and the C_4 carbons of the interior bpys (C(44), C(68)) are separated by only 3.23 Å. Considerable nonplanarity is also exhibited by the N(41) and N(65) pyridine rings, which point into the molecular cavity. The dihedral angle about the central bond, C(34)–C(35), of **2c** is 74°, which is about 10–20° greater than what we estimate for the free ligand, while the dihedral angle of the two distal 5,6-dihydro-1,10-phenanthroline moieties is about 10° due to flattening as a result of complexation.

If we ignore conformational inversion in the dihydrophenanthroline subunits, the complex may be considered as having three chiral centers: one associated with the tetramethylene bridge of the ligand and one on each of the two Ru(bpy)$_2^{2+}$ centers. Of the four diastereomers which are possible for this complex, the X-ray structure indicates formation of the [Δ,*d*,Δ] isomer and its mirror image, [Λ,*l*,Λ]. Examination of a molecular model indicates that the other three diastereomeric forms of the complex would experience considerably greater interaction of their interior bpy's.

Electronic Spectra

The electronic absorption spectra for the series of monometallic complexes [Ru(**2a–c**)(bpy)$_2$](PF$_6$)$_2$ are depicted in Figure 5. We have previously examined complexes such as [Ru(pynap)-(bpy)$_2$]$^{2+}$, where pynap = 2-(2′-pyridyl)-1,8-naphthyridine, and found that the long wavelength absorption, associated with metal–ligand charge transfer (MLCT), is comprised of distinct components which may be assigned to charge transfer from the Ru(II) d-orbital to a π^*-orbital on a specific ligand.[36] Thus the systems under consideration show two MLCT components. The shorter wavelength band appears at 442–446 nm and is associated with MLCT to the bpy ligands. The longer wavelength band occurs at 533, 520, and 514 nm, respectively, for the complexes of **2a–c**. Both the energy and intensity of this second band are consistent with the geometry of the cavity-shaped ligand. As the central polymethylene bridge is lengthened from two to four carbons, the conjugation and resulting electronic delocalization between the bound and unbound pynap moieties decreases. This decrease would raise the energy of the π^* orbital for this ligand and increase the energy of the corresponding MLCT absorption. As the energy for this transition increases, its intensity diminishes with respect to MLCT to the bpy ligands, so that for **2c** the relative intensity of the long wavelength band as compared to the bpy band is less than that for **2a,b**.

The relative contribution of these two MLCT states changes for the dinuclear complexes. Figure 6 depicts the absorption spectra for [(bpy)$_2$Ru(**2b,c**)Ru(bpy)$_2$](PF$_6$)$_4$ compared with those

(34) The narrow temperature range used in this determination somewhat limits its precision.
(35) Thummel, R. P.; Lefoulon, F.; Cantu, D.; Mahadevan, R. *J. Org. Chem.* **1984**, *49*, 2208.
(36) Thummel, R. P.; Decloitre, Y. *Inorg. Chim. Acta* **1987**, *128*, 245.

Table II. Atomic Coordinates (×10⁴) and Equivalent Isotropic Displacement Parameters (Å² × 10³) for $[(bpy)_2Ru(\mathbf{2c})Ru(bpy)_2(PF_6)_4$

atom	x	y	z	U(eq)[a]	atom	x	y	z	U(eq)[a]
Ru(1)	1587(1)	2047(1)	4510(1)	42(1)	C(21)	4766(9)	−579(5)	3473(7)	47(6)
Ru(2)	3724(1)	311(1)	2021(1)	44(1)	C(22)	5664(10)	−925(5)	3538(6)	64(6)
P(1)	7529(4)	1107(2)	1131(3)	70	C(23)	6522(10)	−712(5)	3288(8)	73(8)
F(1)	6604	843	794	129(9)	C(24)	6265(12)	−486(5)	2704(8)	52(7)
F(2)	8453	1370	1468	86(6)	C(25)	6901(11)	−468(6)	2293(9)	72(8)
F(3)	6953	1601	1080	84(6)	C(26)	6634(11)	−236(6)	1776(8)	66(8)
F(4)	8104	612	1183	93(7)	C(27)	5718(12)	−16(5)	1681(7)	57(7)
F(5)	7930	1210	518	105(7)	N(28)	5072(7)	−37(4)	2085(6)	56(5)
F(6)	7128	1003	1744	89(6)	C(29)	5351(11)	−272(5)	2590(7)	43(6)
P(1′)	7473(8)	1122(4)	1172(6)	70	C(30)	4635(10)	−264(5)	3000(6)	32(5)
F(2′)	8545	904	1233	246(22)	N(31)	3845(8)	19(3)	2887(4)	37(4)
F(1′)	6401	1339	1111	282(28)	C(32)	3163(10)	3(5)	3262(7)	36(6)
F(5′)	7244	824	1734	261(31)	N(33)	2409(8)	319(4)	3184(4)	36(4)
F(6′)	7702	1419	610	193(20)	C(34)	1670(10)	294(5)	3497(6)	37(6)
F(3′)	7091	687	757	182(17)	C(35)	855(9)	654(5)	3394(5)	37(6)
F(4′)	7855	1556	1587	216(20)	N(36)	1075(7)	1092(4)	3605(4)	38(4)
P(2)	6930(5)	842(3)	4098(4)	70	C(37)	378(10)	1449(6)	3501(6)	44(6)
F(7)	7090	559	3513	150(12)	N(38)	592(7)	1899(4)	3753(4)	38(4)
F(8)	6770	1125	4684	167(13)	C(39)	5(10)	2276(6)	3598(6)	45(6)
F(9)	5911	1036	3790	146(11)	C(40)	286(11)	2727(5)	3877(7)	46(6)
F(10)	7948	648	4406	143(10)	N(41)	2728(8)	2139(5)	4043(5)	54(5)
F(11)	7463	1296	3865	207(14)	C(42)	2916(11)	2524(6)	3726(7)	64(7)
F(12)	6396	387	4332	176(12)	C(43)	3800(14)	2622(6)	3502(7)	89(8)
P(2′)	6910(7)	880(4)	4024(5)	70	C(44)	4519(14)	2297(7)	3623(7)	105(10)
F(7′)	7240	744	3415	89(10)	C(45)	4384(10)	1860(6)	3910(6)	72(7)
F(8′)	6570	1022	4657	149(18)	C(46)	3442(11)	1793(6)	4130(6)	56(6)
F(9′)	5823	711	3819	104(11)	C(47)	3175(11)	1365(5)	4458(6)	40(6)
F(10′)	7997	1050	4228	114(10)	C(48)	3775(10)	955(6)	4562(6)	59(6)
F(11′)	6644	1404	3782	125(11)	C(49)	3423(12)	578(5)	4892(6)	66(7)
F(12′)	7176	357	4266	113(10)	C(50)	2520(12)	612(6)	5099(6)	59(7)
P(3)	925(4)	1489(2)	−2097(3)	70	C(51)	1971(10)	1025(6)	4967(6)	59(6)
F(13)	1541	1410	−2635	143(9)	N(52)	2286(8)	1394(4)	4664(5)	43(5)
F(14)	309	1567	−1558	167(10)	N(53)	583(9)	1922(4)	5100(6)	51(5)
F(15)	−51	1510	−2541	215(14)	C(54)	−333(13)	1771(5)	4985(6)	62(7)
F(16)	1901	1476	−1651	147(9)	C(55)	−965(11)	1690(5)	5407(10)	78(8)
F(17)	1048	2052	−2154	142(9)	C(56)	−630(14)	1779(6)	5995(9)	80(8)
F(18)	802	925	−2038	141(11)	C(57)	312(13)	1934(5)	6135(7)	73(7)
P(3′)	976(11)	1471(5)	−1904(6)	70	C(58)	915(11)	2007(5)	5685(8)	53(7)
F(13′)	1688	1506	−2402	67(10)	C(59)	1931(12)	2155(5)	5803(8)	55(7)
F(14′)	263	1436	−1406	90(12)	C(60)	2483(15)	2230(5)	6365(7)	82(9)
F(15′)	98	1659	−2359	68(10)	C(61)	3441(14)	2398(6)	6398(9)	92(9)
F(16′)	1854	1283	−1449	117(16)	C(62)	3842(12)	2481(6)	5913(9)	79(8)
F(17′)	1237	2008	−1712	78(10)	C(63)	3300(12)	2412(5)	5365(7)	62(7)
F(18′)	714	935	−2096	239(48)	N(64)	2367(9)	2252(3)	5304(5)	47(5)
P(4)	3374(4)	−1931(2)	3113(3)	70	N(65)	4308(10)	971(4)	2260(5)	59(5)
F(19)	4002	−1575	2765	138(10)	C(66)	5235(12)	1091(6)	2413(7)	74(8)
F(20)	2747	−2288	3460	130(9)	C(67)	5629(14)	1555(7)	2426(9)	105(10)
F(21)	2765	−2085	2508	186(11)	C(68)	5004(17)	1904(8)	2328(9)	134(12)
F(22)	3985	−1777	3717	136(8)	C(69)	3981(16)	1817(7)	2211(7)	104(10)
F(23)	2612	−1515	3186	149(9)	C(70)	3620(14)	1335(7)	2191(7)	76(8)
F(24)	4137	−2348	3040	154(10)	C(71)	2549(12)	1194(7)	2068(6)	63(7)
P(4′)	3406(8)	−2034(4)	3123(5)	70	C(72)	1710(16)	1488(6)	2016(7)	97(9)
F(19′)	3833	−2395	2679	187(21)	C(73)	806(13)	1277(9)	1876(8)	110(11)
F(20′)	2980	−1673	3567	107(11)	C(74)	711(14)	802(7)	1786(7)	89(9)
C(21′)	3485	−1608	2669	118(14)	C(75)	1555(13)	522(5)	1857(6)	65(7)
F(22′)	3328	−2460	3577	135(14)	N(76)	2447(8)	710(5)	1997(4)	47(5)
F(23′)	2330	−2146	2826	117(12)	N(77)	2996(7)	−288(5)	1661(6)	58(6)
F(24′)	4483	−1922	3421	109(11)	C(78)	2724(11)	−656(6)	1943(7)	72(7)
N(1)	996(8)	2722(4)	4332(5)	45(5)	C(79)	2129(14)	−1035(8)	1702(8)	109(11)
C(2)	1247(10)	3137(6)	4602(7)	55(6)	C(80)	1859(16)	−1022(7)	1138(14)	145(15)
C(3)	830(12)	3564(6)	4400(8)	66(7)	C(81)	2137(12)	−673(8)	768(8)	103(9)
C(4)	130(12)	3577(5)	3911(9)	73(8)	C(82)	2749(11)	−283(7)	1046(8)	73(8)
C(5)	−175(10)	3159(7)	3650(7)	56(7)	C(83)	3158(12)	144(7)	761(10)	73(8)
C(6)	−930(11)	3116(5)	3085(7)	79(8)	C(84)	3048(13)	211(9)	173(11)	124(13)
C(7)	−1545(10)	2650(5)	3094(6)	71(7)	C(85)	3439(18)	614(11)	−37(10)	155(16)
C(8)	−891(11)	2204(5)	3197(6)	51(7)	C(86)	3973(17)	953(9)	305(12)	147(14)
C(9)	−1159(9)	1755(6)	2982(6)	56(6)	C(87)	4052(11)	863(7)	906(9)	83(9)
C(10)	−534(10)	1351(6)	3120(6)	46(6)	N(88)	3667(9)	471(6)	1130(5)	57(5)
C(11)	−734(10)	877(6)	2928(6)	53(6)	C(89)	1841(25)	2495(12)	9821(14)	116(12)
C(12)	−58(10)	521(5)	3081(6)	43(6)	C(90)	2723(25)	2284(11)	9782(13)	80(10)
C(13)	−319(10)	20(6)	2914(7)	75(8)	N(91)	3426(19)	2136(9)	9846(11)	93(9)
C(14)	−797(11)	−238(6)	3393(8)	89(8)	C(92)	422(12)	834(7)	−45(9)	108(15)
C(15)	−126(12)	−459(6)	3899(8)	102(9)	C(93)	678	637	−580	108(14)
C(16)	663(10)	−128(5)	4243(6)	70(7)	C(94)	565	138	−691	104(15)
C(17)	1593(10)	−66(5)	3935(6)	44(6)	C(95)	196	−164	−267	125(14)
C(18)	2410(11)	−361(5)	4059(6)	50(6)	C(96)	−60	34	268	143(36)
C(19)	3214(10)	−326(5)	3740(6)	42(6)	C(97)	53	533	379	98(13)
C(20)	4057(11)	−626(4)	3838(6)	47(6)	C(98)	542	1371	74	136(16)

[a] Equivalent isotropic U defined as one-third of the trace of the orthogonalized U_{ij} tensor.

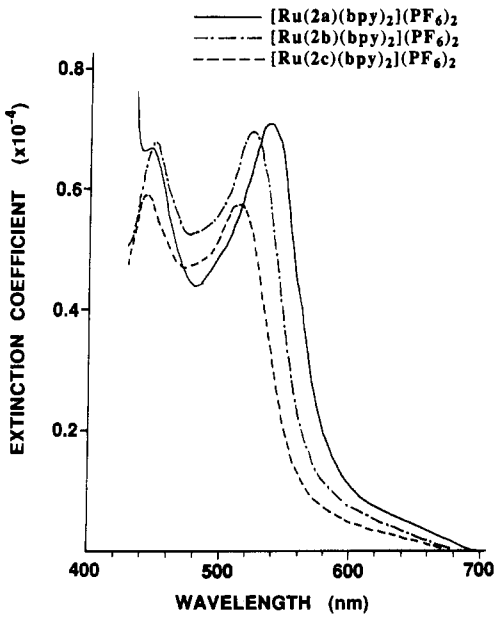

Figure 5. Electronic absorption spectra of $[Ru(\mathbf{2a}–\mathbf{c})(bpy)_2](PF_6)_2$ complexes, 10^{-4} M in CH_3CN.

Table III. Selected Bond Lengths, Bond Angles, and Torsion Angles for $[(bpy)_2Ru(\mathbf{2c})Ru(bpy)_2](PF_6)_4$

	Bond Lengths (Å)		
Ru(1)–N(1)	2.035(12)	Ru(1)–N(38)	2.078(9)
Ru(1)–N(41)	1.981(11)	Ru(1)–N(52)	2.035(11)
Ru(1)–N(53)	2.031(13)	Ru(1)–N(64)	2.037(11)
Ru(2)–N(28)	2.048(10)	Ru(2)–N(31)	2.086(10)
Ru(2)–N(65)	2.019(11)	Ru(2)–N(76)	2.040(12)
Ru(2)–N(77)	2.031(12)	Ru(2)–N(88)	2.037(12)
	Bond Angles (deg)		
N(38)–Ru(1)–N(1)	79.4(4)	N(31)–Ru(2)–N(28)	77.6(5)
N(52)–Ru(1)–N(41)	79.9(5)	N(76)–Ru(2)–N(65)	80.3(5)
N(64)–Ru(1)–N(53)	78.3(5)	N(88)–Ru(2)–N(77)	79.9(6)
	Torsion Angles (deg)		
C5–C6–C7–C8	−53.2	C24–C29–C30–C21	−15.6
C8–C39–C40–C5	−16.7	N28–C29–C30–N31	−8.9
N38–C39–C40–N1	−10.9	N65–C70–C71–N76	−5.0
N53–C58–C59–N1	8.4	C69–C70–C71–C72	−7.7
C57–C58–C59–C60	2.9	N77–C82–C83–N88	−2.5
N41–C46–C47–N52	−4.9	C81–C82–C83–C84	−3.9
C45–C46–C47–C48	−4.4	C17–C34–C35–C12	−74.9
C21–C22–C23–C24	−45.2	N33–C34–C35–N36	−73.8

of the analogous mononuclear complexes. The electronegativity of the bridging ligand will now be affected by the presence of the second $Ru(bpy)_2^{2+}$. With two metal centers undergoing a d-π^* transition into the same bridging ligand, the intensity of this transition will *decrease* as the conjugation between the two pynap halves of the molecule increases. Therefore the relative intensity of the long to short wavelength components of the $[(bpy)_2Ru(\mathbf{2b,c})Ru(bpy)_2](PF_6)_4$ MLCT state is *less* for **2b** than for **2c** due to better delocalization in the more planar bridging ligand **2b**.

Figure 7 depicts the electronic absorption spectra of $[(bpy\text{-}d_8)_2Ru(\mathbf{2c})Os(bpy\text{-}d_8)_2](PF_6)_4$ and its two mononuclear analogs. The absorption bands for the dinuclear complex approximate a summation of the curves for the two mononuclear systems with the maximum of the long wavelength component at 522 nm being intermediate between the mononuclear bands at 514 and 541 nm. As noted for the homodinuclear Ru(II) complex, the relative contribution of the low-energy MLCT state is diminished from what is predicted by a simple additivity effect.

The emission spectra for the mononuclear complexes $[Ru(\mathbf{2a}–\mathbf{c})(bpy)_2](PF_6)_2$ were measured in acetonitrile at 298 K and are presented in Figure 8. All three systems emit strongly with

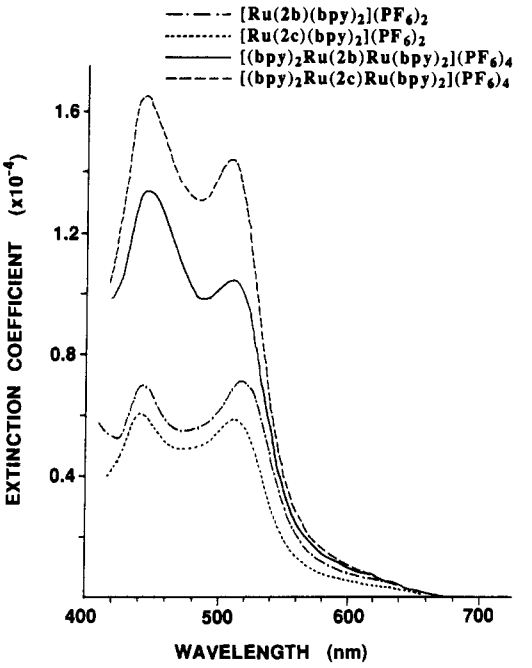

Figure 6. Electronic absorption spectra of mono- and dinuclear $Ru(bpy)_2^{2+}$ complexes of **2b,c**, 10^{-4} M in CH_3CN.

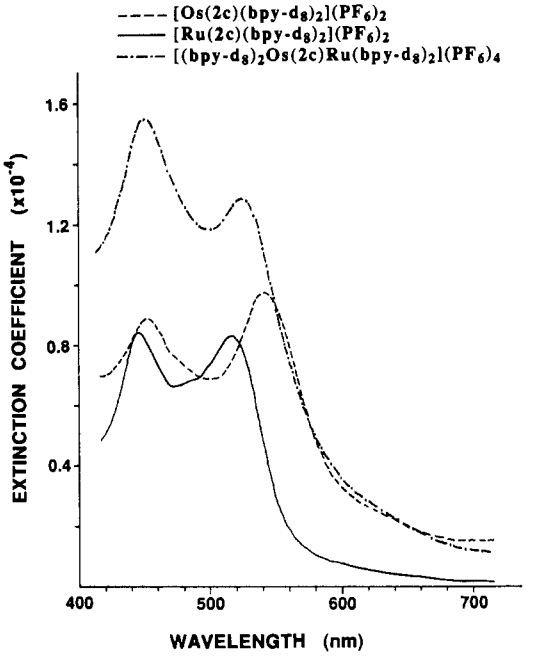

Figure 7. Electronic absorption spectra of $Os(bpy\text{-}d_8)_2^{2+}$ and $Ru(bpy\text{-}d_8)_2^{2+}$ complexes of **2c** and the dinuclear Os(II)–Ru(II) complex of **2c**, 10^{-4} M in CH_3CN. The Os complexes show an additional weak absorption at ca. 790 nm.

maxima observed at 775, 739, and 738 nm for **2a–c**, respectively. Compared to the analogous emission for $Ru(bpy)_3^{2+}$, which occurs at 615 nm, the observed red shift is consistent with emission from the lower energy MLCT state associated with the more delocalized cavity-shaped ligand **2**. As the length of the polymethylene bridge decreases, causing the ligand to become more planar, the emission intensity decreases. A possible interpretation would require the two pynap components of **2a–c** to act independently of one another such that MLCT into the metal-bound pynap might be quenched to some extent by the unbound pynap. Better conjugation between these two halves of the molecule as in **2a** would lead to more efficient quenching and diminished luminescence.

A very weak emission was observed for $[Os(\mathbf{2c})(bpy\text{-}d_8)_2](PF_6)_2$ at 720 nm. The energy of this emission is in the range expected

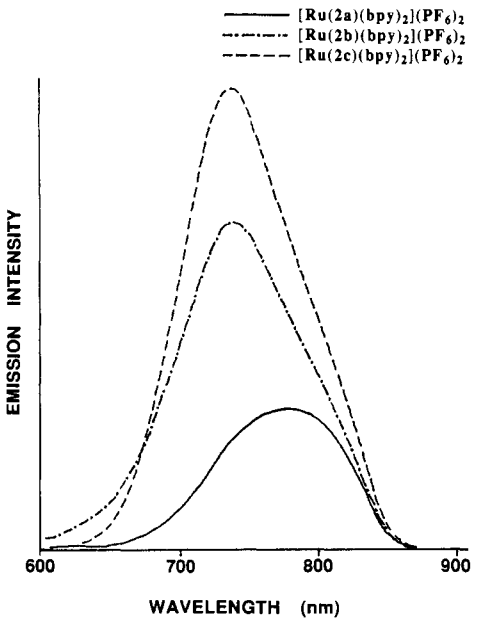

Figure 8. Uncorrected luminescence spectra of $[Ru(\mathbf{2a}–\mathbf{c})(bpy)_2](PF_6)_2$ at 298 K, 10^{-4} M in CH_3CN with excitation at 525 nm.

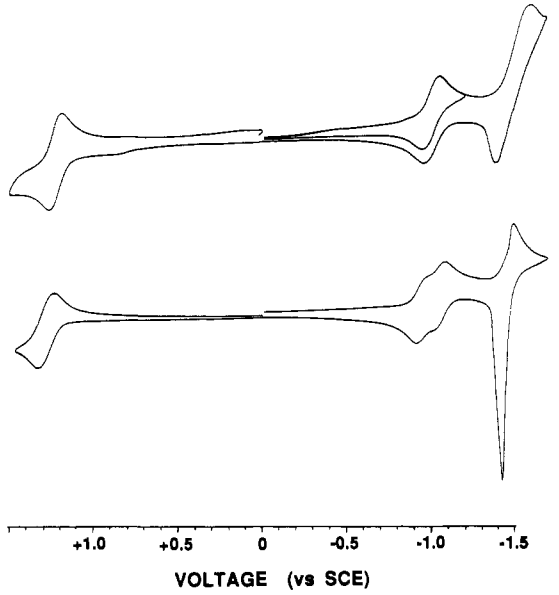

Figure 9. Cyclic voltammograms of $[Ru(\mathbf{2c})(bpy)_2](PF_6)_2$ (top) and $[(bpy)_2Ru(\mathbf{2c})Ru(bpy)_2](PF_6)_4$ (bottom) in CH_3CN containing 0.1 M TBAP at 25 °C with a scan rate of 200 mV/s. The top CV shows a small wave at ca. +0.8 V, which may represent a slight impurity.

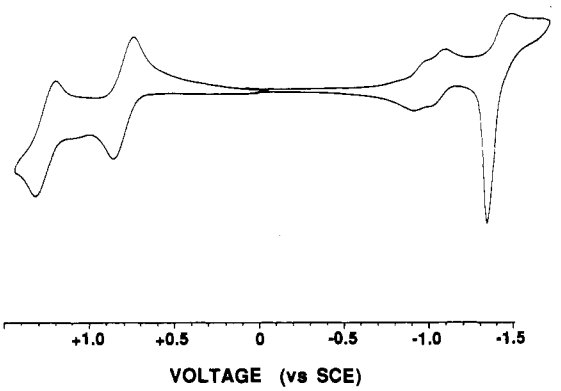

Figure 10. Cyclic voltammogram of $[(bpy\text{-}d_8)_2Ru(\mathbf{2c})Os(bpy\text{-}d_8)_2](PF_6)_4$ in CH_3CN containing 0.1 M TBAP at 25 °C with a scan rate of 200 mV/s.

for mixed-ligand Os polypyridine complexes.[37] The fact that it is blue-shifted with respect to the corresponding Ru(II) complex is more difficult to understand.

The homodinuclear complex $[(bpy)_2Ru(\mathbf{2c})Ru(bpy)_2](PF_6)_4$ showed a considerably weaker emission at 732 nm with about 15% the intensity of its mononuclear counterpart, while the heterodinuclear complex $[(bpy\text{-}d_8)_2Ru(\mathbf{2c})Os(bpy\text{-}d_8)_2](PF_6)_4$ gave a barely perceptible band at 720 nm with about 30% the intensity of the mononuclear Os complex. The apparent quenching of the normally intense Ru(II) MLCT state by the Os(II) center was further probed by a control experiment involving an equimolar mixture (5×10^{-5} M CH_3CN) of $[Ru(\mathbf{2c})(bpy\text{-}d_8)_2](PF_6)_2$ and $[Os(\mathbf{2c})(bpy\text{-}d_8)_2](PF_6)_2$. The emission from the Ru(II) complex decreased to 82% indicating that some energy transfer could be involved in the quenching process. However, a ligand-mediated process, as was suggested for the mononuclear complexes of **2a–c**, appears to be predominant.

Redox Behavior

We have previously examined the redox behavior of the complex $[Ru(pynap\text{-}2)(bpy)_2](PF_6)_2$, where pynap-2 = (3,3′-dimethylene)-pynap.[36] For this complex we observe the first reduction wave at –0.99 V and the Ru^{2+}/Ru^{3+} oxidation at +1.22 V (vs SCE). The mononuclear complexes $[Ru(\mathbf{2a}–\mathbf{c})(bpy)_2](PF_6)_2$ all contain the pynap-2 structural unit, and their redox properties are all quite similar and well behaved, showing first reduction potentials of –0.90, –0.98, and –1.00 V and oxidation potentials of +1.25, +1.24, and +1.22 V for the complexes containing **2a–c**, respectively. Since the first reduction corresponds to the addition of an electron to the π^* orbital of the large cavity ligand, the trend toward more negative potential with increasing length of the polymethylene bridge is consistent with raising the energy of the π^* orbital of this ligand. The oxidation potential corresponds to the removal of an electron from a d-orbital of the metal, and much less variation is observed.

Dodsworth and Lever have established a correlation between the ground-state redox potentials of ruthenium polypyridine complexes and their lowest energy excited state.[38] The differences between the half-wave potentials for the first reduction and first oxidation of **2a–c** are 2.15, 2.22, and 2.22 V and the maxima for their emission bands appear at 1.60, 1.68, and 1.68 eV, respectively. These data correlate well with a linear relationship established for a variety of Ru(II) polypyridine complexes and verify the LMCT nature of the emitting state.

The cyclic voltammograms for the dinuclear complex $[(bpy)_2Ru(\mathbf{2c})Ru(bpy)_2](PF_6)_4$ and its mononuclear analog $[Ru(\mathbf{2c})(bpy)_2](PF_6)_2$ are illustrated in Figure 9. For the dinuclear complex, a single quasi-reversible[39] oxidation wave appears at +1.28 V implying that both Ru(II) centers loose an electron at the same potential. This result contrasts other dinuclear Ru(II) complexes where more metal–metal communication is observed and splitting of the oxidation wave occurs.[13] The first reduction, on the other hand, is split into two waves with half-wave potentials of –0.95 and –1.05 V. Since this reduction is ligand based, the implication is that the two halves of **2c** are reduced independently but influence one another. If the two pynap-2 moieties of the dinuclear complex were completely independent, then both reductions would occur at the same potential and a single wave would appear. Instead the first reduction is shifted slightly positive by the presence of a second Ru(II) in the complex and the second

(37) Kober, E. M.; Carpar, J. V.; Lumpkin, R. S.; Meyer, T. J. *J. Phys. Chem.* **1986**, *90*, 3722.
(38) Dodsworth, E. S.; Lever, A. B. P. *Chem. Phys. Lett.* **1986**, *124*, 152.
(39) Electrochemical reversibility was judged on the basis of the following criteria: the separation of the anodic and cathodic peak potentials equals $60/n$ mV, where n is the number of electrons transferred; the ratio of the anodic and cathodic peak currents is unity.[40]
(40) Bard, A. J.; Faulkner, L. R. *Electrochemical Methods, Fundamentals and Applications*; Wiley: New York, 1980; p 228.

potential is shifted slightly negative since it involves the addition of a second electron to the bridging ligand **2c**. This behavior is consistent with the relative intensities of the MLCT absorptions discussed earlier. The shape of the second reduction wave implies that the addition of a third electron to the complex affords a species which evidences strong adsorption to the electrode surface.

The cyclic voltammogram for the heterodinuclear complex $[(bpy)_2Ru(\mathbf{2c})Os(bpy)_2](PF_6)_4$ is shown in Figure 10. Two reversible oxidation waves are observed as +0.81 and +1.26 V, which compare well with the potentials for the corresponding Os(II) (+0.78) and Ru(II) (+1.22) mononuclear complexes, again indicating that these centers are acting independently. The first reduction is likewise split into two waves at −0.96 and −1.04 V, bearing a strong resemblance to the homodinuclear system.

Acknowledgment. We are grateful to the Robert A. Welch Foundation and the National Science Foundation (Grant CHE-8910991) for financial support of this work. The NMR spectrometer was partially funded by the NSF (Grant CHE-8616352). We thank Dr. James Korp for the X-ray structure determination, Dr. Brian Chait for the electrospray mass spectra, Dr. Hugh Webb for the HRMS, and the reviewers for insipirational comments. C.H. thanks Elf Aquitaine and the French Ministry of Foreign Affaires for a Bourse Lavoisier.

Supplementary Material Available: Tables pertinent to the X-ray crystallographic determination of $[(bpy)_2Ru(\mathbf{2c})Ru(bpy)_2](PF_6)_4$ including data collection and processing parameters (Table S1), anisotropic displacement parameters (Table S2), bond lengths (Table S3), bond angles (Table S4), and H-atom coordinates (Table S5) and a figure displaying the emission response curve for the R928 PMT (9 pages). Ordering information is given on any current masthead page.